



Molecular dynamics simulations of nanoparticle growth ... and beyond

Pascal Brault

*GREMI, UMR7344 CNRS Université d'Orléans,
Orléans, France*

pascal.brault@univ-orleans.fr

<http://www.univ-orleans.fr/gremi/pascal-brault>





Outline

- Practical MD simulations
- Supported nanoparticle growth
- Free nanoparticle growth in a Gas Agregation Source
- Hydrocarbon plasma soot growth
- MD simulations of plasma processing as a whole
- Conclusions/Future works



Practical Molecular Dynamics simulation

- ✓ Calculate all trajectories of a set of atoms, molecules, ...
via the Newton equation of motion
→ Suitable for processes at nanoscale (up to 10^9 atoms)

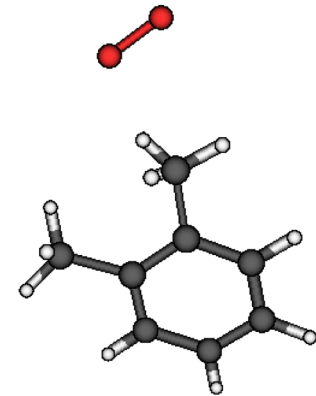
$$\vec{F}_i = m_i \vec{a}_i = m_i \frac{d\vec{v}_i}{dt} = m_i \frac{d^2 \vec{r}_i}{dt^2}$$

and

$$\vec{F}_i = -\vec{\nabla}_{\vec{r}_i} U(\vec{r}_1, \vec{r}_2, \vec{r}_3, \dots, \vec{r}_N)$$

- ✓ A rigorous approach requires the use of robust interaction potentials and initial conditions (positions, velocities) preferably matching experimental conditions
→ appropriate velocity distribution functions can be derived from experimental conditions.

- ✓ Proper energy dissipation:
 - Energy release during bond formation : deposition, bond formation/breaking
 - Annealing→ via friction term(s), thermostat(s)





Practical Molecular Dynamics simulation

Relevance/significance of MD Simulations

Flux :

Exp. $1 \cdot 10^{15} \text{cm}^{-2} \text{s}^{-1} = 10 \text{ species} / \text{nm}^2 / \text{s}$ - MD 1 specie / $10 \times 10 \text{ nm}^2 / 2 \text{ ps}$

Prohibit long time diffusion, except if including specific strategies (fbMC, CVHD, hyperdynamics, ...)

Pressure/simulation box size

Solid density : Pt 65 nm^{-3}

Liquid density: water 33 nm^{-3}

→ Can be treated. Diffusion coefficients can be calculated without additional approximation(s)

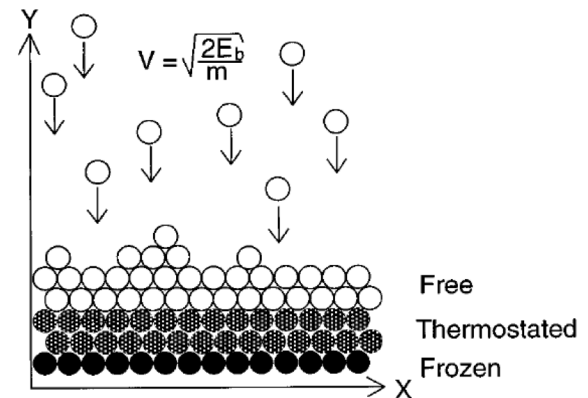
Gas density : 1 atm = $2.4 \cdot 10^{-2} \text{ nm}^{-3}$ → Not enough species in box of size d at pressure P

Solution: relevant parameter = Collision number $\propto P \cdot d$

→ $\uparrow P \downarrow d$ should work.

Thermal relaxation

- Choose a relevant specie release time: i.e. greater than thermalisation time
- Choose a relevant thermostat (region i.e. what should be thermostated) within this relevant time
- For interactions with surface, one can guess that only the substrate should be thermostated





Practical Molecular Dynamics simulation: Interactions potentials

Metals : Embedded Atom Method (EAM)

- ⇒ energy of a solid is a unique functional of the electron density.
- ⇒ uses the concept of electron (charge) density to describe metallic bonding:
- ⇒ each atom contributes through a spherical, exponentially-decaying field of electron charge, centered at its nucleus, to the overall charge density of the system.
- ⇒ Binding of atoms is modelled as embedding these atoms in this “pool” of charge, where the energy gained by embedding an atom at location r is some function of the local density.

⇒ The total energy thus writes:

$$E_{pot} = \sum_{i=1}^N E_i = \frac{1}{2} \sum_{i=1}^N \sum_{j, j \neq i}^N \phi_{ij}(r_{ij}) + \sum_{i=1}^N F_i(\rho_i) \quad \rho = \sum_{j, j \neq i}^N f_i(r_{ij}) \quad f(r) = \frac{f_e \exp\left[-\beta\left(\frac{r}{r_e} - 1\right)\right]}{1 + \left(\frac{r}{r_e} - \lambda\right)^{20}}$$

With pairwise function:

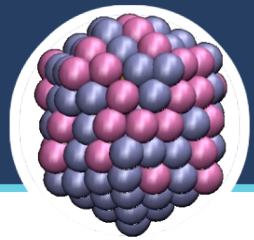
$$\phi(r) = \frac{A \exp\left[-\alpha\left(\frac{r}{r_e} - 1\right)\right]}{1 + \left(\frac{r}{r_e} - \kappa\right)^{20}} - \frac{B \exp\left[-\beta\left(\frac{r}{r_e} - 1\right)\right]}{1 + \left(\frac{r}{r_e} - \lambda\right)^{20}}$$

and mixing rule:

$$\phi^{ab}(r) = \frac{1}{2} \left[\frac{f^b(r)}{f^a(r)} \phi^{aa}(r) + \frac{f^a(r)}{f^b(r)} \phi^{bb}(r) \right]$$

S.M. Foiles, M.I. Baskes Contributions of the embedded-atom method to materials science and engineering, MRS Bulletin, 37 (2012) 485-491.

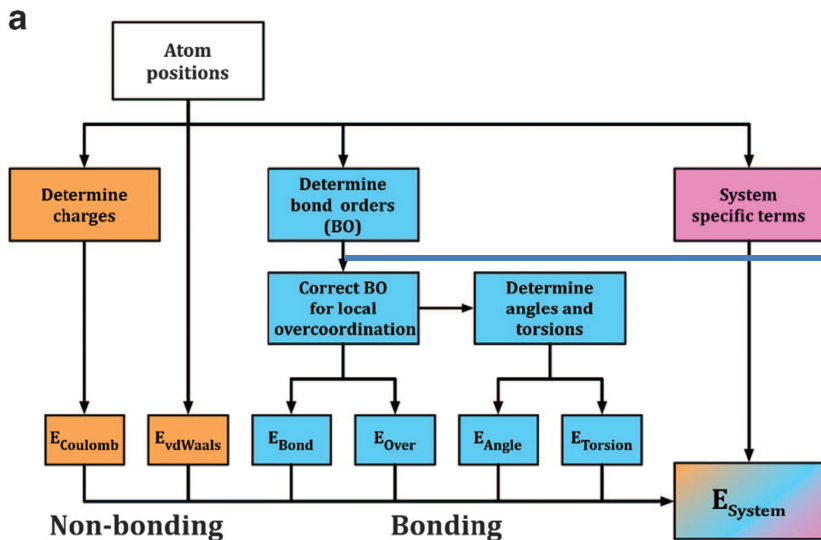
X. W. Zhou et al, Misfit energy-increasing dislocations in vapor-deposited CoFe/NiFe multilayers, Phys. Rev. B 69 (2004) 144113



Practical Molecular Dynamics simulation: Interactions potentials

ReaxFF allows for computationally efficient simulation of materials under realistic conditions, *i.e.* bond breaking and formation with accurate chemical energies. It also includes variable partial charges.

Due to the chemistry, ReaxFF has a complicated potential energy function: $E_{\text{system}} = E_{\text{bond}} + E_{\text{over}} + E_{\text{angle}} + E_{\text{tors}} + E_{\text{vdWaaals}} + E_{\text{Coulomb}} + E_{\text{Specific}}$



$$\begin{aligned}
 \text{BO}_{ij} &= \text{BO}_{ij}^{\sigma} + \text{BO}_{ij}^{\pi} + \text{BO}_{ij}^{\pi\pi} \\
 &= \exp \left[p_{\text{bo}1} \left(\frac{r_{ij}}{r_o^{\sigma}} \right)^{p_{\text{bo}2}} \right] + \exp \left[p_{\text{bo}3} \left(\frac{r_{ij}}{r_o^{\pi}} \right)^{p_{\text{bo}4}} \right] \\
 &\quad + \exp \left[p_{\text{bo}5} \left(\frac{r_{ij}}{r_o^{\pi\pi}} \right)^{p_{\text{bo}6}} \right]
 \end{aligned}$$

Correct Bond Order \Rightarrow Correct description of reaction energy barriers

Overview of the ReaxFF total energy components

TP Senftle et al, *The ReaxFF reactive force-field: development, applications and future directions*, npj Computational Materials 2, (2016) 15011



Supported Pt₂PdAu nanocatalyst growth on porous carbon: Pt, Pd, Au co-deposition

Potentials used in the system:

Pt-Pd-Au: EAM potentials

C – C: Tersoff potential -> thermostat

Metal – C: LJ potential (Steele)

Model porous carbon from TEM measurements

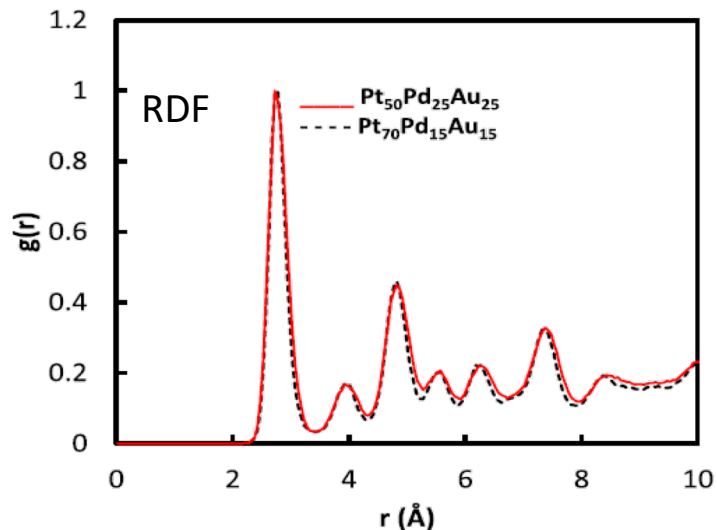
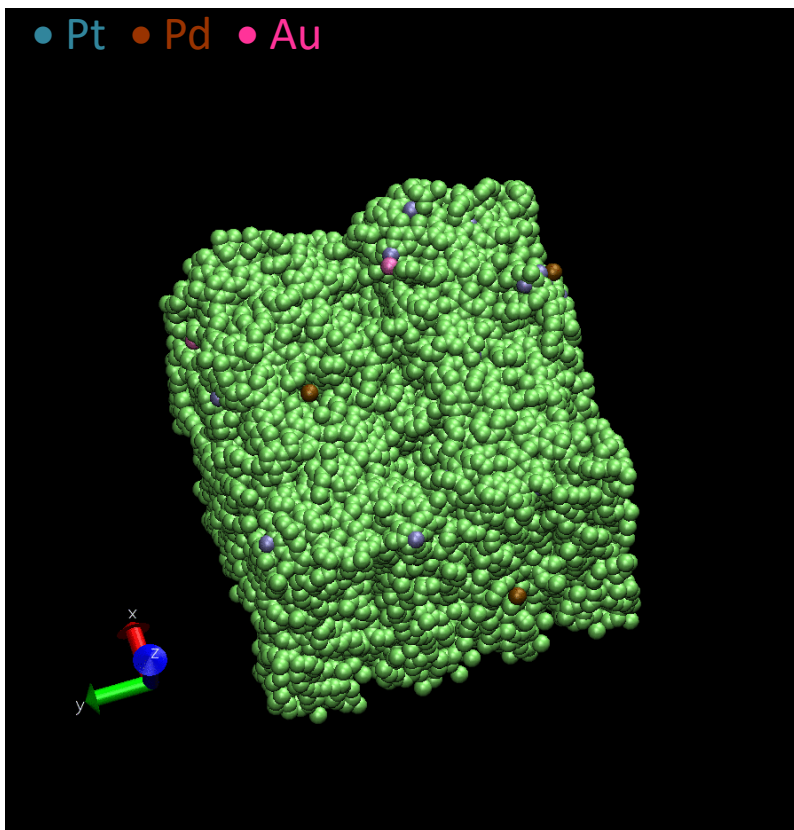


Table 1 – EAM and average experimental surface energies of the low index faces of Pt, Pd, Au in Jm^{-2} [40].

	Pt	Pd	Au
(111)	1.44	1.22	0.79
(100)	1.65	1.37	0.92
(110)	1.75	1.49	0.98
Experimental, face averaged	2.49	2.00	1.5

■ Gold surface segregation

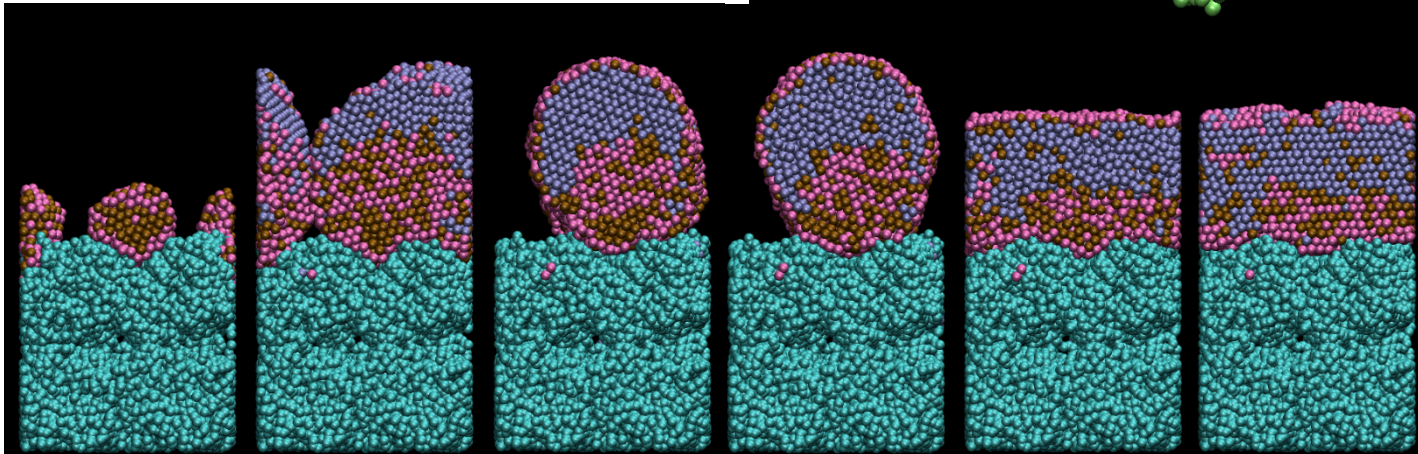
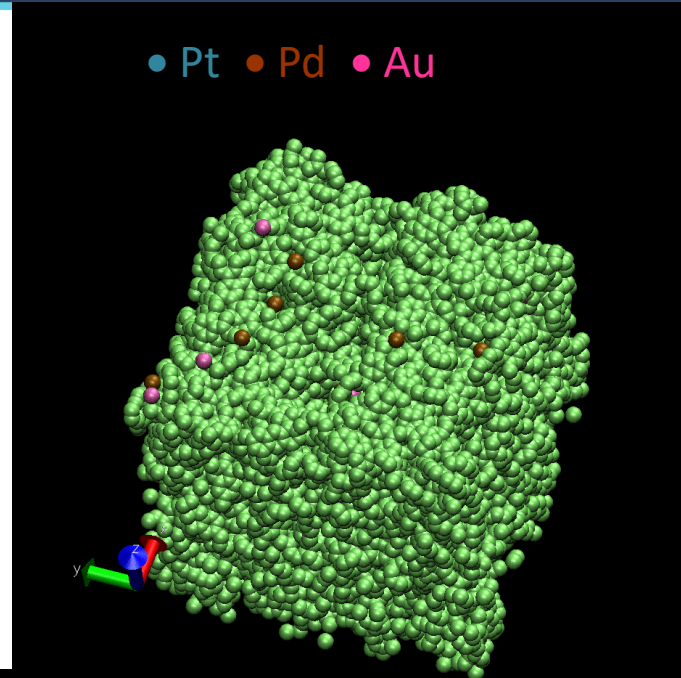
P. Brault, Molecular dynamics simulations of ternary Pt_xPd_yAu_z fuel cell nanocatalyst growth, International Journal of Hydrogen Energy 41 (2016) 22589-22597



Supported Pt₂PdAu nanocatalyst growth on porous carbon: Sequential PdAu deposition followed by Pt deposition

→ AuPd@Pt₂ core@shell

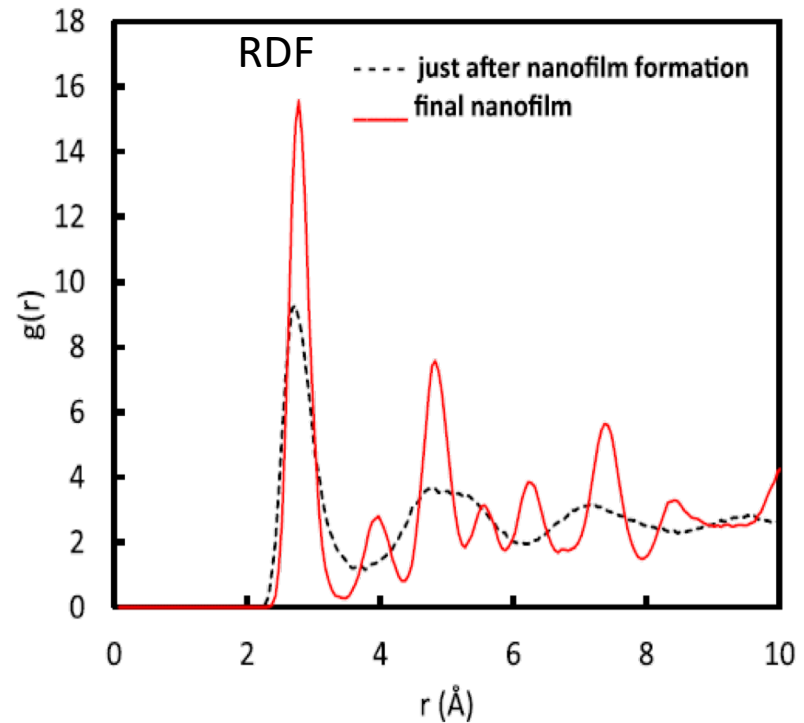
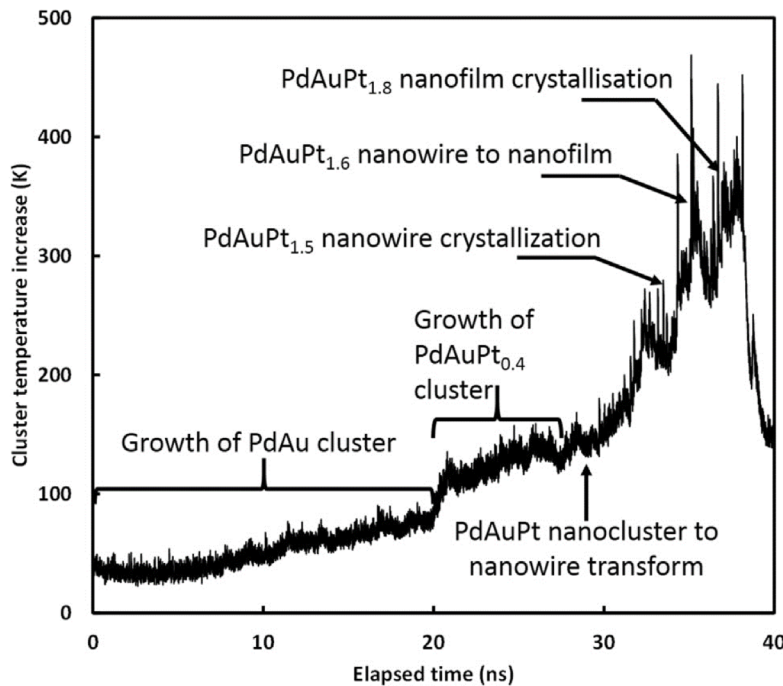
But always Au segregation towards surface!





Molecular dynamics simulation of sputtering plasma catalysts growth: Supported Pt₂PdAu nanocatalyst growth on porous carbon

Correlations between cluster temperature evolution and morphology transform in the course of deposition of core-shell PdAu@Pt₂ nanocatalyst

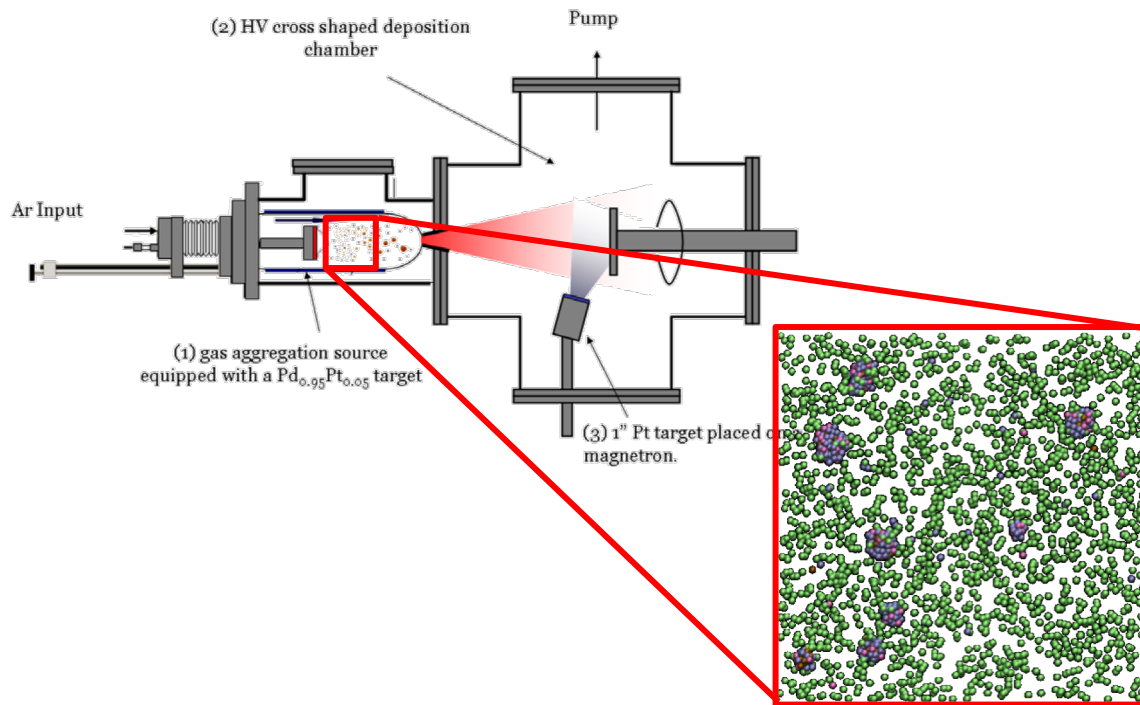


- L. Xie, P. Brault, C. Coutanceau, A. Caillard, J. Berndt, E. Neyts Appl. Cat. B, 62 (2015) 21 – 26
- P. Brault, et al, International Journal of Hydrogen Energy 41 (2016) 22589-22597
- E. Neyts, P. Brault, Plasma Processes and Polymers 14 (2017) 1600145 - FP7 FCH-JU SMARTCat project #325327



Free nanoparticle growth in a Gas Aggregation Source

Gas aggregation source: simulation principles



Matching experimental and simulation conditions

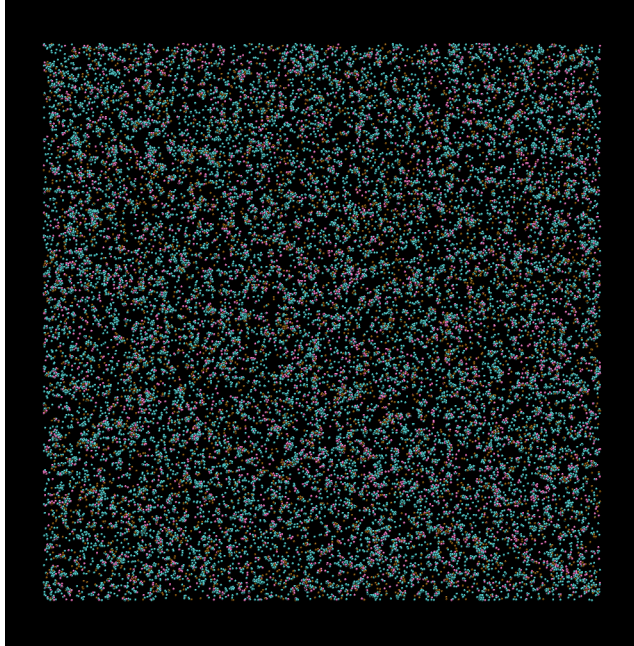
- Metal vapor density in the aggregation chamber

$$N_M = (Y_{Ar} I / q) / (\Phi(Ar) \cdot P_{at} / P_{Ar})$$
 → will give the proper ratio of N_M/N_{Ar} in the simulation box
- Collision number identical in experiments and in simulation
 i.e. $P_{exp} \cdot d_{exp} = P_{sim} \cdot d_{sim}$

A. Caillard et al, *PdPt catalyst synthesized using a gas aggregation source and magnetron sputtering for fuel cell electrodes*, J. Phys. D: Appl. Phys. 48 (2015) 475302
 E Quesnel et al *Modeling metallic nanoparticle synthesis in a magnetron-based nanocluster source by gas condensation of a sputtered vapor*, J. Appl. Phys. 107 (2010) 054309



Free $\text{Pt}_3\text{Me}(\text{Au})$ (Me = Ni, Cu) nanocatalyst growth



Tricks :

NVE ensemble for Pt, Ni and Au

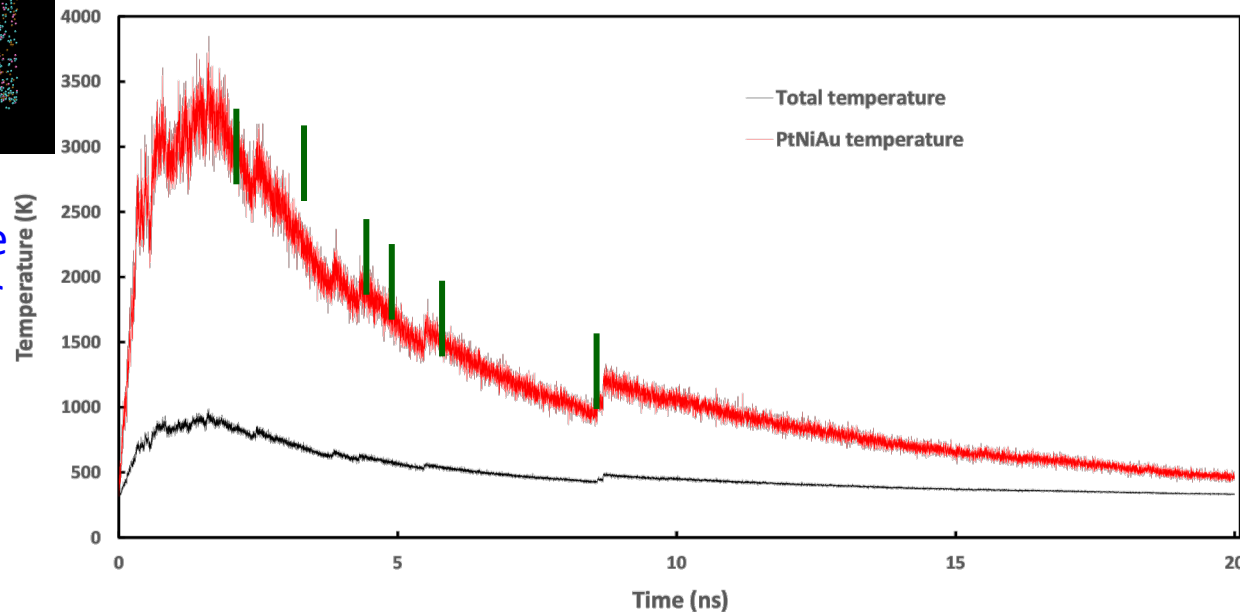
NVT ensemble for Ar : surrounding gas is the thermostat

Ratio of N_{Ar} to N_{metal} estimated from experiments: depends on discharge current, Ar pressure, ...

here: $N_{\text{Ar}}=128000$; $N_{\text{Pt}}=19200$; $N_{\text{Ni}}=6400$; $N_{\text{Au}}=6400$

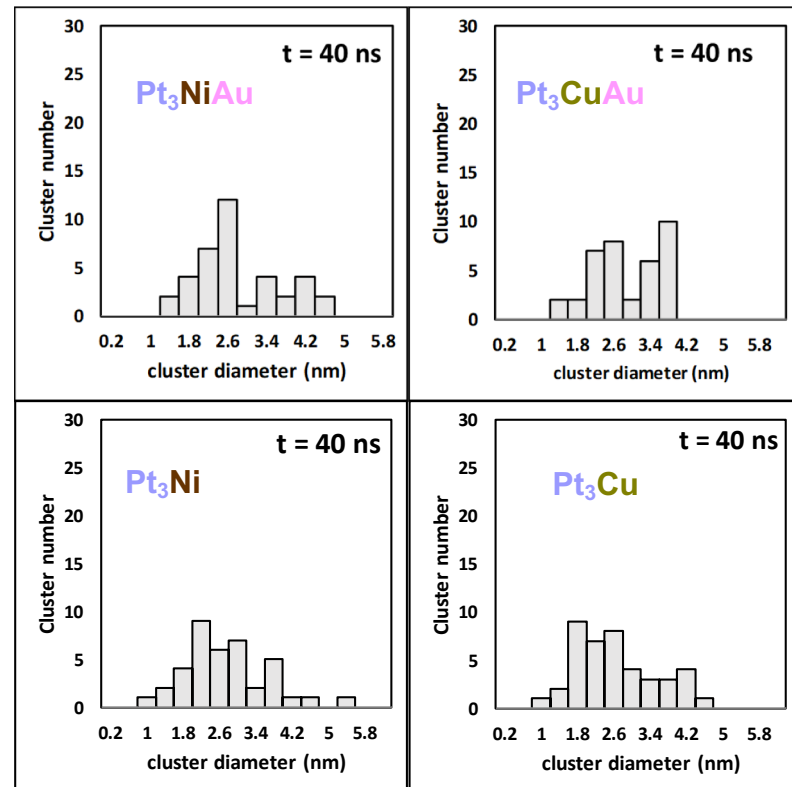
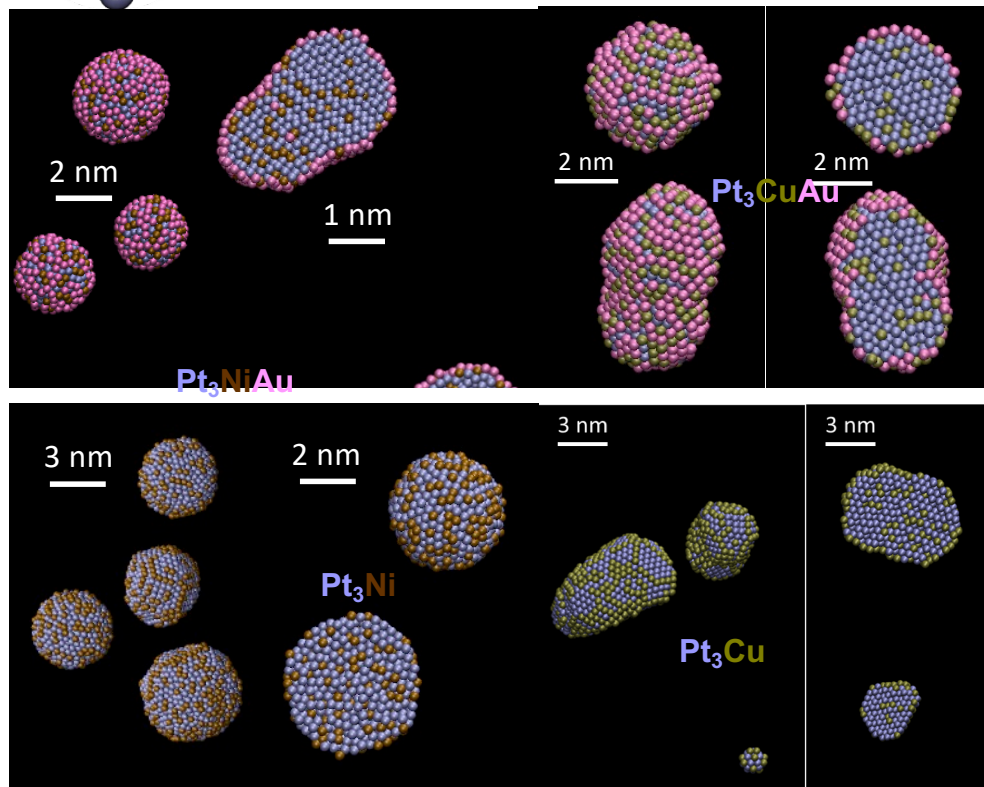
Box size $64 \times 64 \times 64 \text{ nm}^3$; $dt = 1 \text{ fs}$, $4 \cdot 10^7$ timesteps

Temperature evolution of the vapor and of the metal vapor and then of clusters the \rightarrow cluster growth and coalescence : breaks in the plot (green vertical sticks)



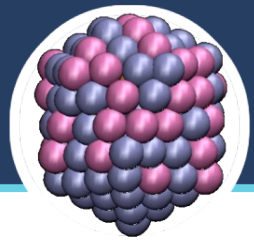


Free Pt₃Me(Au) (Me = Ni, Cu) nanocatalyst growth



- Au segregation towards cluster surface
- CuAu surface alloy for Pt₃CuAu → better efficiency for Oxygen Reduction Reaction
- Pt₃Cu(Au) more well crystallized

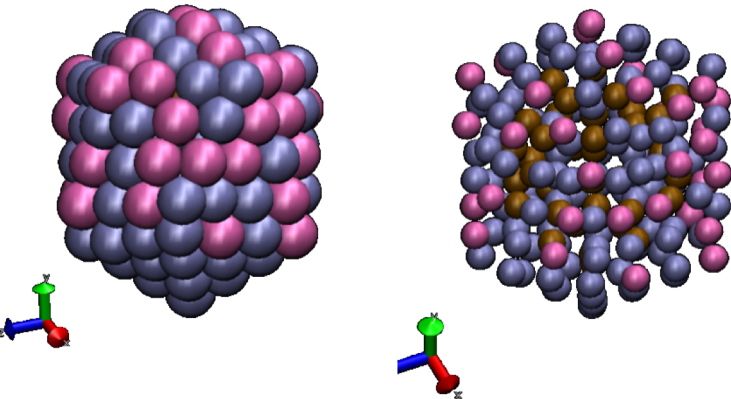
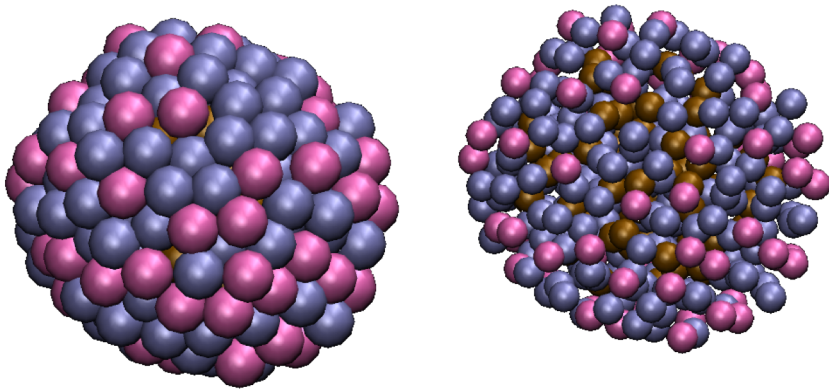
P. Brault, et al, Pt₃MeAu (Me = Ni, Cu) fuel cell nanocatalyst growth, shapes and efficiency: A molecular dynamics simulation approach, *J. Phys. Chem. C* 123 (2019) 29656 – 29664



Free Pt₃Me(Au) (Me = Ni, Cu) nanocatalyst growth

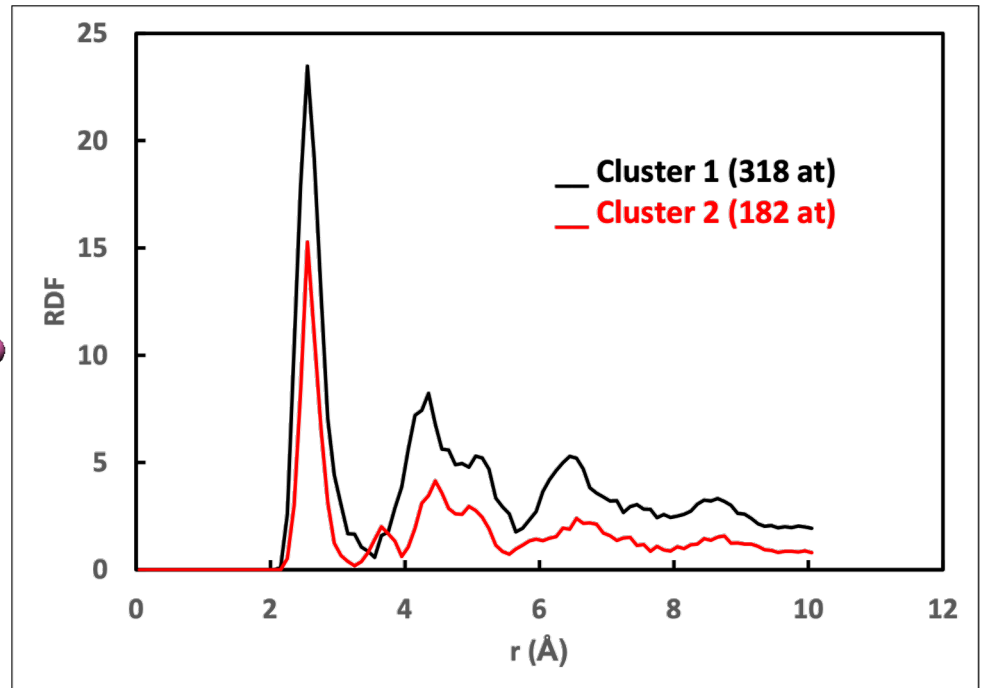
Cluster 1 (318 at.) : cuboctahedron ?

Pt₁₈₉Ni₆₂Au₆₇ ≈ Pt₃NiAu ● Pt; ● Ni; ● Au

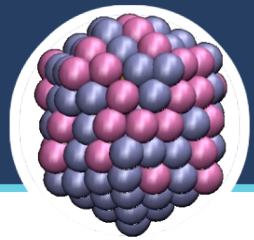


Cluster 2 (182 at.) : icosahedron ?

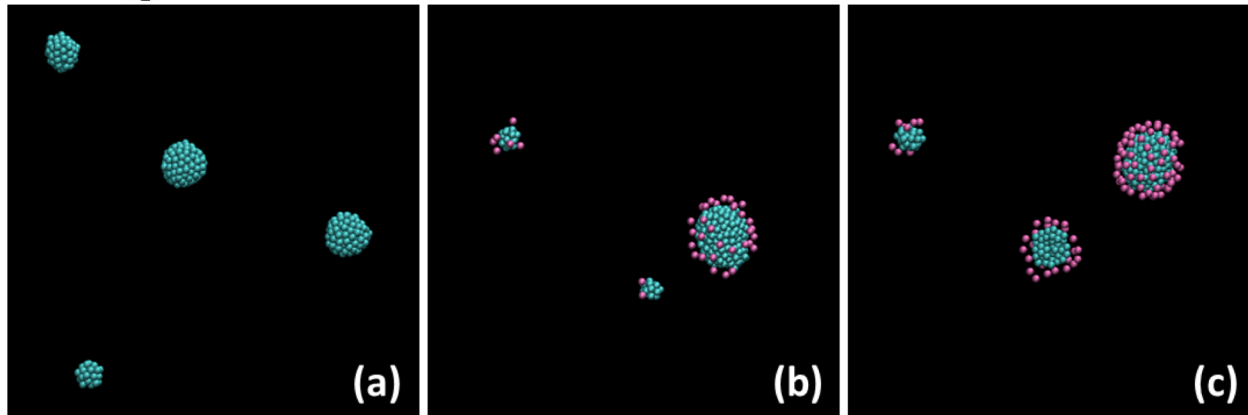
Pt₁₁₁Ni₃₈Au₃₃



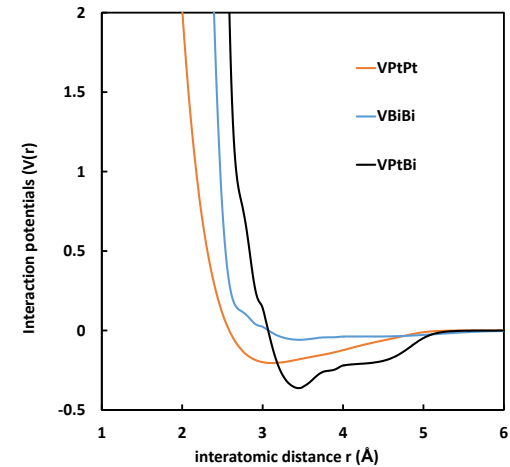
	1 st NN	2 nd NN	3 rd NN
Theoretical (fcc) 0.6Pt+0.2Ni+0.2Au	2.738 Å	3.872 Å	4.74 Å
Cluster 1	2.55 Å	(3.75 Å)	4.35 Å
Cluster 2	2.55 Å	3.65 Å	4.45 Å



Pt_xBi_y nanocatalyst growth



Snapshot of the final clusters at 20 ns. Argon atoms (4000) are not represented for clarity. $n_{Pt} + n_{Bi} = 500$. (a) Pt alone (b) Pt₉Bi₁ (c) Pt₈Bi₂. Box size 16x16x16 nm³



Plots of the pair part of the EAM interaction potentials:

$$V_{PtPt}(r), V_{BiBi}(r), V_{PtBi}(r).$$

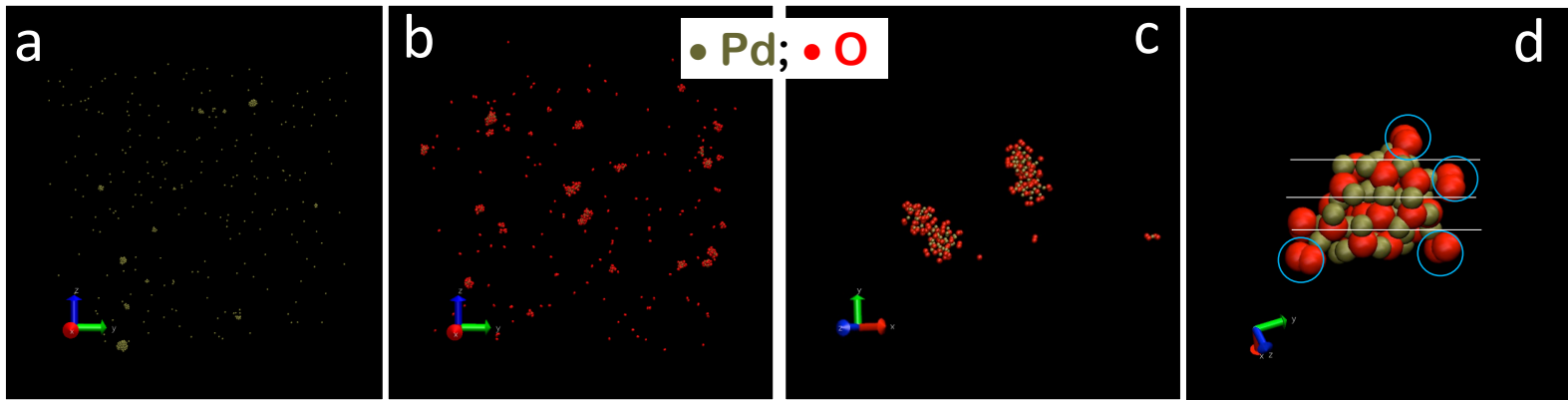
- Cluster atomic arrangements are typical of a crystalline structure of the Pt cores, with numbers of 1st nearest neighbors between 10 and 12 (i.e. consistent with fcc arrangement)
- Bi composition < 20% leads to cluster surfaces with both Pt and Bi, allowing catalytic activity enhancement.
- Pt/Bi atomic composition is not only globally preserved, but is also verified for each cluster

B.S.R. Kouamé et al, Insights on the unique electro-catalytic behavior of PtBi/C materials, *Electrochimica Acta* 329 (2020) 135161



Reactive free PdO nanocatalyst growth

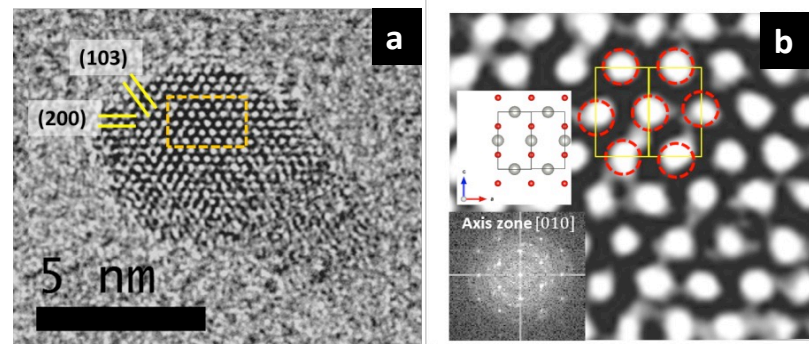
ReaxFF reactive variable charge potentials for Pd sputtering in Ar-O₂ gas mixture



Snapshot of (a-b) the overall Pd and PdO clusters at 25 ns simulation time (c-d) of the detailed PdO clusters.

First results: O addition -> no more free Pd, more PdO than Pd clusters

■ GAS Experiments, W. Chamorro-Coral et al



Ratio of N_{Ar} to N_{metal} estimated from experiments = 40 here;
 $N_{Ar} = 20000$; $N_{Pd} = 500$; $N_{O} = 1000$; Box size : 40 x 40 x 40 nm³
 Integration time 0.25 fs → 1. 10⁸ iterations

Potential ReaxFF : T. Senftle et al, J. Chem Phys 139 (2013) 044109

P. Brault et al. , Frontiers in Chemical Science and Engineering Frontiers of Chemical Science and Engineering 13 (2019) 324 – 329

W. Chamorro-Coral et al, Plasma Processes and Polymers 16 (2019) e1900006



Hydrocarbon plasma and soots

μ wave plasma $H_2/10\% CH_4$
Initial conditions for MD simulations
from 0D model (*)

	1450 K	1650 K	1950K
H_2 (*)	1000	1000	1000
H	7	30	100
CH_4	200	100	100
$\bullet CH_3$	2	5	7
C_2H_4	50	20	3
C_2H_2	400	500	600

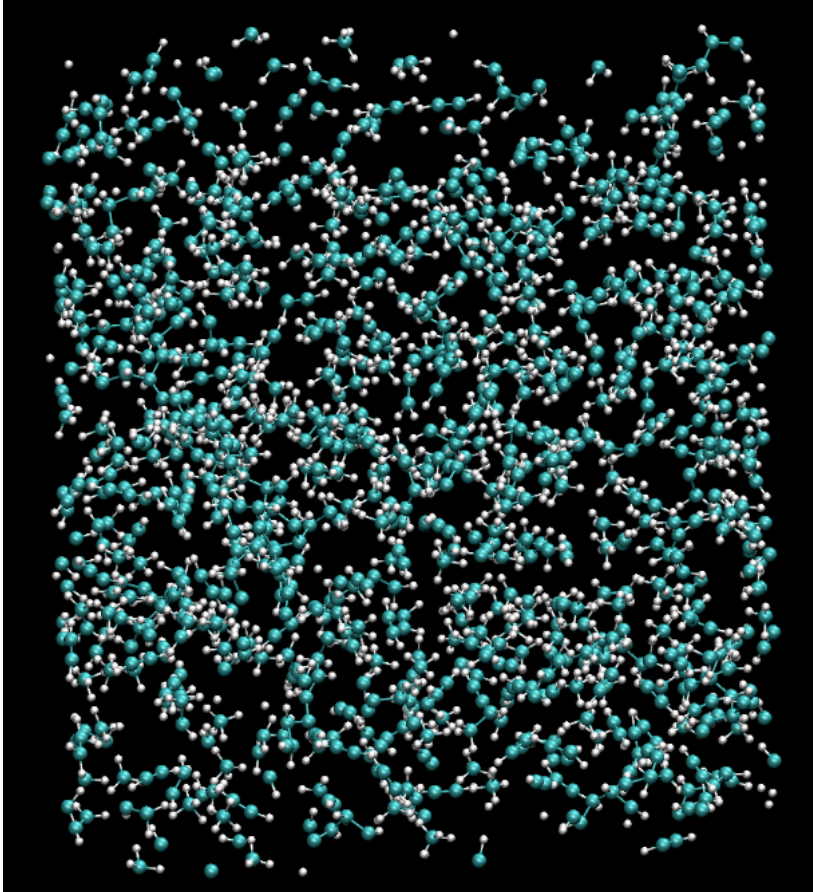
(*) au lieu de 10000
Suffisant pour thermostat

- Reactions can freely occur
- Bond formation energy is transported to walls by H_2 buffer gas, as in experiment (96% of molecules are H_2). H atoms from H_2 are thermostated.



Hydrocarbon plasma and soots

1450 K



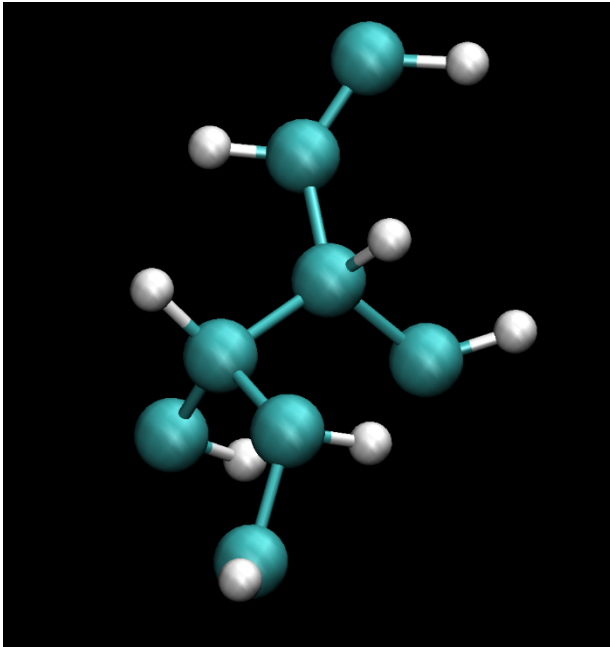
- ReaxFF potential
- NVT for H_2 \rightarrow thermostat
- NVE for other species
- $4 \times 4 \times 4 \text{ nm}^3$
- $dt = 0.25 \text{ fs}$; 10^7 timesteps
- 300h on 8 core Intel Xeon



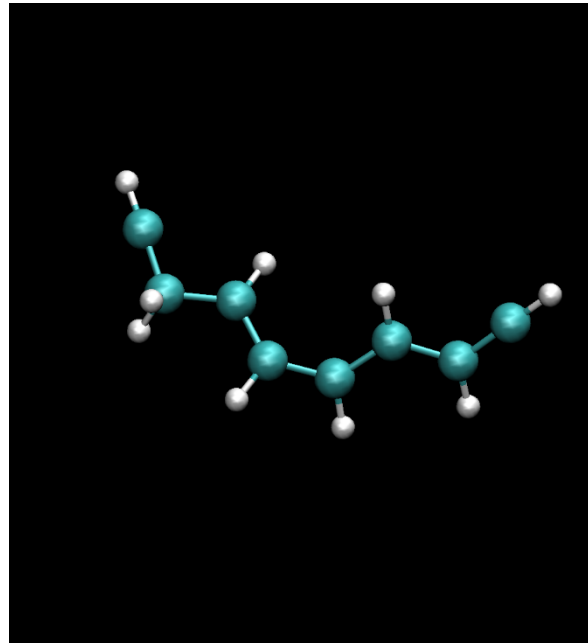
Hydrocarbon plasma and soots

1450 K

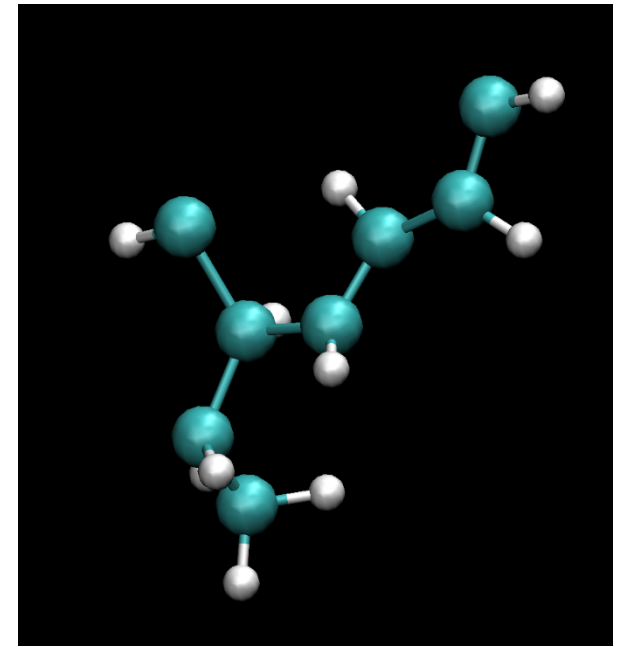
■ Negatively charged ions



#2603
 $q = -0.45$



#2004
 $q = -0.2$



#3088
 $q = -0.25$



Hydrocarbon plasma and soots

1450 K

	H2	H	CH4	CH3	C2H4	C2H2						
initial molar fraction	94%	0.07%	2.00%	0.02%	0.50%	4.00%						
# initial molecules SB	1000	7	200	2	50	400						
	C1	C2	C3	C4	C5	C6	C7	C8	C9	C10	C11	C12
initial #molecules	202	450	0	0	0	0	0	0	0	0	0	0
final #molecules	201	330	6	15	4	9	1	5	1	1	1	1
initial #Cx	202	900	0	0	0	0	0	0	0	0	0	0
final #Cx	201	660	18	60	20	54	7	40	9	10	11	12
final fraction Cx	18.24%	59.89%	1.63%	5.44%	1.81%	4.90%	0.64%	3.63%	0.82%	0.91%	1.00%	1.09%



Hydrocarbon plasma and soots

1650 K

	H2	H	CH4	CH3	C2H4	C2H2						
initial molar fraction	94.00%	0.30%	1.00%	0.05%	0.20%	5.00%						
# initial molecules SB	1000	30	100	5	20	500						
	C1	C2	C3	C4	C5	C6	C7	C8	C9	C10	C11	C12
initial #molecules	105	520	0	0	0	0	0	0	0	0	0	0
final #molecules	114	380	13	19	4	15	0	3	0	1	0	1
initial #Cx	105	1040	0	0	0	0	0	0	0	0	0	0
final #Cx	114	760	39	76	20	90	0	24	0	10	0	12
final fraction Cx	9.96%	66.38%	3.41%	6.64%	1.75%	7.86%	0.00%	2.10%	0.00%	0.87%	0.00%	1.05%



Hydrocarbon plasma and soots

1950 K

	H2	H	CH4	CH3	C2H4	C2H2						
initial molar fraction	93.00%	1.00%	0.30%	0.07%	0.03%	6.00%						
# initial molecules SB	1000	100	100	7	3	600						
	C1	C2	C3	C4	C5	C6	C7	C8	C9	C10	C11	C12
initial #molecules	107	603	0	0	0	0	0	0	0	0	0	0
final #molecules	121	415	18	40	3	13	0	2	1	0	0	0
initial #Cx	107	1206	0	0	0	0	0	0	0	0	0	0
final #Cx	121	830	54	160	15	78	0	16	9	0	0	0
final fraction Cx	9.43%	64.69%	4.21%	12.47%	1.17%	6.08%	0.00%	1.25%	0.70%	0.00%	0.00%	0.00%



MD simulations of plasma processing as a whole

1/ recovering/scaling experimental conditions

Hypothesis : Collision number are the same in experiments and simulations so, $P_{exp}d_{exp} = P_{sim}d_{sim}$ thus $N_{sim} = \frac{P_{exp}}{k_B T_g} \cdot S_{sim} \cdot d_{exp}$ and if r_{cut} is the largest cutoff radius : $d_{sim} > \frac{N_{sim}}{S_{sim}} \cdot r_{cut}^3$

(S_{sim} is the chosen smallest area of the simulation box)

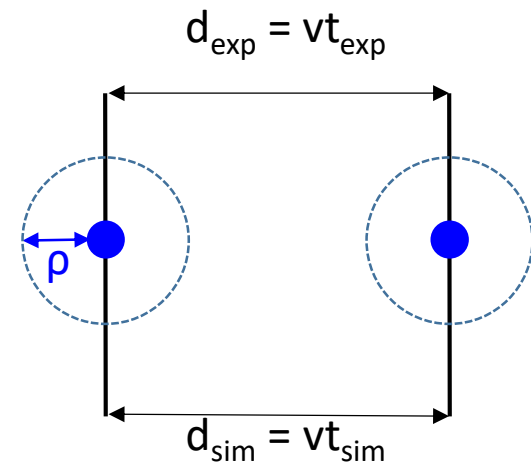
2/ experimental time recovery

Velocities are same in exp and simulations

$$v = \frac{d_{exp}}{t_{exp}} = \frac{d_{sim}}{t_{sim}}, \text{ when } d_{exp}, d_{sim} > 2\rho$$

$$\text{then, } t_{exp} = \frac{d_{exp}}{d_{sim}} \cdot t_{sim}, \text{ when } d_{exp}, d_{sim} > 2\rho$$

$$\text{or, } t_{exp} = t_{sim}, \text{ when } d_{exp}, d_{sim} \leq 2\rho$$





MD simulations of plasma processing as a whole

New reactive and including electron interaction potential allow targeting multiscale MD simulations of operating plasma reactor

2/ combine improved force fields

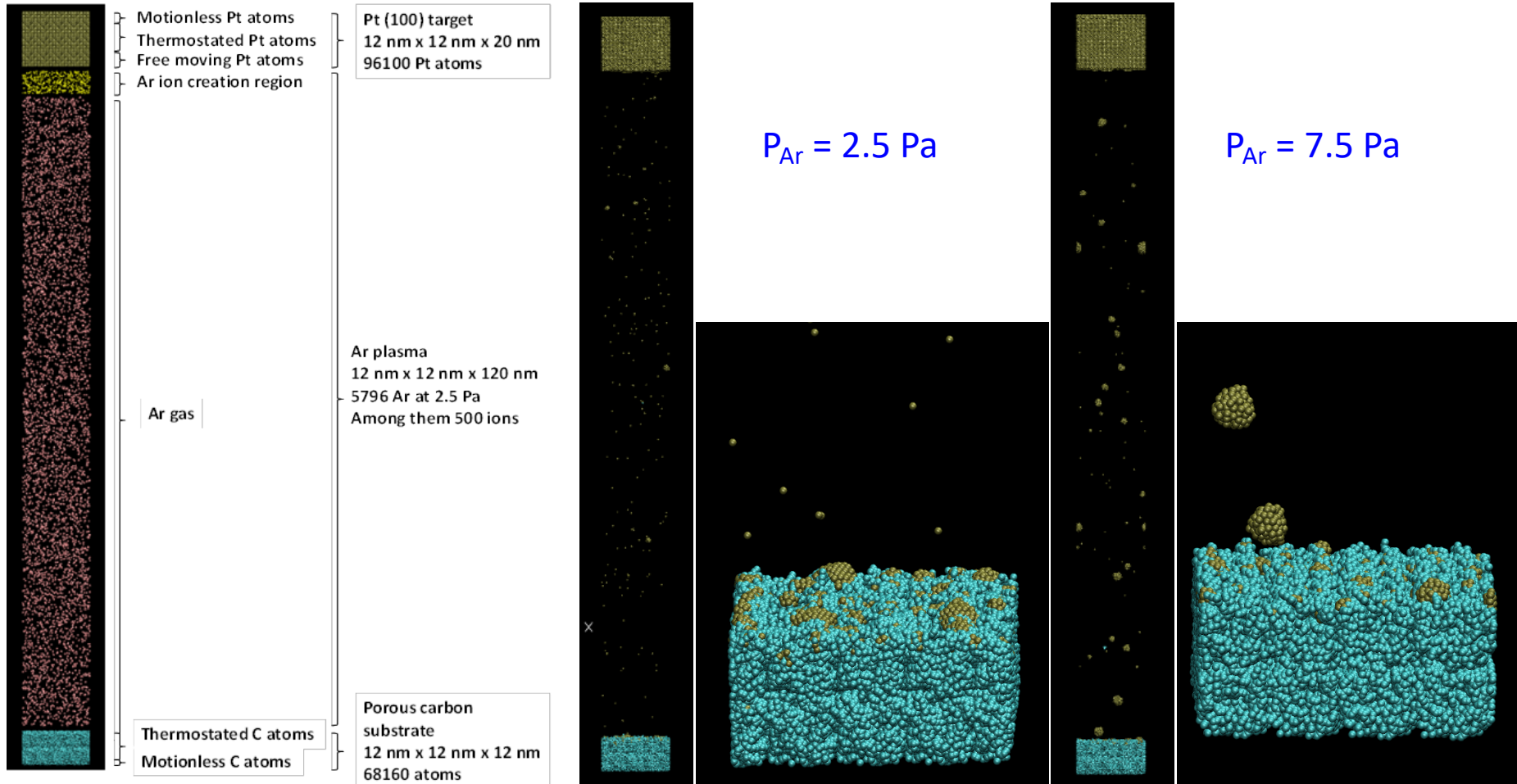
Plasma factor	Possible?	Example
electric field	yes	CNT growth
atoms and hyperthermal species	yes	Si-NW oxidation
radicals	yes	a-C:H growth
ions	yes	sputtering
electronically excited states	yes	etching
vibrationally excited states	yes / no (reaxFF)	/
photons	implicit	(polymer degradation)
electrons	Yes (eFF, e-reaxFF)	/

E. Neyts, P. Brault (Review article), *Molecular dynamics simulations for plasma surface interactions*, *Plasma Processes and Polymers* 14 (2017) 1600145



MD simulations of plasma processing as a whole

Application to nanocluster growth in plasma sputtering



P. Brault, *Multiscale Molecular Dynamics Simulation of Plasma Processing: Application to Plasma Sputtering*, Front. Phys. 6 (2018) 59



Conclusions

- MD simulations of supported and free metal alloy nanoparticle provides insight of surface composition : for Pt alloy this is well correlated with experiments on catalytic performance, especially when adding Au (expected to stabilize clusters).
- Reactive MD is very powerful since availability of reactive and variable charge reaxFF potential family. Growth of free PdO clusters is well compared with GAS experiments.
- Matching experimental conditions is a condition for successful comparisons.
- Full plasma processing modelling is reachable by MD simulations provided a cutoff distance is defined for scaling down the experimental reactor size



Future works

■ Nanocatalysts

- ❑ Non Platinum Group Catalysts for fuel cell operation TiO_{2-x} , ZrO_{2-x}
- ❑ GAS growth and reactivity \rightarrow OH adsorption

■ Plasma – liquid interactions

- ❑ RONS action on Endocrine Disruptive Chemicals, Pharmaceutical residues.

■ Plasma chemistry

- ❑ Including electrons in plasma chemistry using MD



Acknowledgements

Many thanks for your attention

Many thanks to people who contribute to the works

Staff members	PhD Candidates	Postdoc	Collaborations
Anne-Lise Thomman	Aboubakr Ennadjaoui (+)	Hervé Rabat	C. Charles, R. Boswell
Amaël Caillard	Sujuan Wu	Marjorie Cavarroc	C. Coutanceau
Yves Tessier	Mathieu Mougnot	William Chamorro-Coral	C. Corr, D. Ramdutt
Thomas Lecas	Lu Xie	Vanessa Orozco-Montes	D. B. Graves
Johannes Berndt	Stéphane Cuyenet	Glenn Otakandza	E. Neyts
	Sotheara Chuon		P. & C. Andreazza